Monocytic Microparticles (mMP) derived from different monocyte subsets display similar morphology and size

Mohd Nor Ridzuan Abd Mutalib, Siti Zulaiha Marhalim, Nurhidanatasha Abu Bakar, Maryam Azlan*

School of Health Sciences, Universiti Sains Malaysia, Health Campus, 16150 Kubang Kerian Kelantan, Malaysia.

Abstract

Microparticles (MP) derived from monocytes are known as monocytic microparticles (mMP). To date, the morphology of microparticles (MP) derived from different monocyte subsets, $CD14^+$ monocytes and $CD16^+$ monocytes is still unclear. Therefore, the morphology and size of mMP derived from both monocytes were assessed. Monocyte subsets were isolated by immunomagnetic selection followed by lipopolysaccharide stimulation and subsequently mMP were isolated by ultracentrifugation. Our data have shown that mMP appear as a single particle with no variation in size. In conclusion, mMP derived from different monocyte subsets exhibit similar morphology and size despite their antigenic differences.

Keywords: monocytic microparticles, monocyte subsets, scanning electron microscope, dynamic light scattering

Article Info

Received 17th February 2020
Accepted 17th March 2020
Published 1st April 2020
*Corresponding author: Maryam Azlan; e-mail: maryamazlan@usm.my

ISSN: 1823-7010, eISSN: 2600-7444

Introduction

Microparticles (MP) are one of the extracellular vesicles that play important role in intercellular communication and possibly biomarkers for disease diagnosis [1]. MP are heterogeneous in size and are found in various body fluids [2]. Following cell stimulation, a redistribution of lipids occur which lead to MP formation and release through budding [3]. MP are also released by platelets, endothelial cells as well as monocytes [4].

Human blood monocytes consist of the classical $CD14^{++}CD16^{-}$ monocytes, intermediate $CD14^{+}CD16^{+}$ monocytes and non-classical $CD14^{+}CD16^{++}$ monocytes [5]. Different monocyte subsets play different role such as the classical monocytes are highly phagocytic and are known to be important scavenger cells while the intermediate monocytes are involved in proliferation and stimulation of T cells [6]. In the presence of stimuli such as lipopolysaccharide (LPS), calcium ionophore, histamine, and P-selection, monocytes secrete monocytic microparticles (mMP). It has been suggested that mMP released by different monocyte subsets would eventually play different role in the immune system [1].

Previous study has identified the morphology of MP derived from B-lymphocytes by scanning electron microscopy (SEM) [7] but not MP derived from monocytes. Other study has shown that the combination of transmission electron microscope (TEM) and SEM, platelet-derived MP were diverse in size, shape and density [8]. On the other hand, dynamic light scattering (DLS) were used to compare between the polydispersity of homogenous and heterogeneous population of platelets in the presence of MP [9]. The size of MP derived from platelets was less than 1000 nm as determined by DLS [10]. Although the size of mMP derived from THP-1 cells has been previously identified [11], the size of mMP derived from primary monocyte subsets is unknown. Therefore, this is the first study performed to determine the morphology and size of MP derived from $CD14^{+}$ monocytes and $CD16^{+}$ monocyte subsets.

Materials and methods

Monocyte subsets isolation

Human blood samples were collected from healthy donors with appropriate informed consent as approved by the Research Ethics Committee (Human) USM (USM/JEPeM/15040128). Healthy donors of 21 to 45 years old were selected with no previous history of serious medical conditions and are not on medication. Briefly, 10 ml of blood were collected from each donor (5-10 donors). PBMC were isolated by density gradient centrifugation using lymphocyte separation medium (Corning), washed with 1X PBS (Amresco) before being resuspended in appropriate buffer or media.

Isolation of human whole blood monocytes from peripheral blood mononuclear cells (PBMC) was performed using Human Pan Monocyte Isolation Kit (Miltenyi Biotec) according to the manufacturer's protocol. Further isolation was performed to purify $CD14^{+}$ monocytes and $CD16^{+}$ monocytes from the whole monocytes using $CD16^{+}$ Monocyte Isolation Kit (Miltenyi Biotec). $CD14^{+}$ monocytes and $CD16^{+}$ monocytes were isolated from the negative and positive fractions respectively.

Monocytic microparticles (mMP) isolation

Whole monocytes, $CD14^+$ monocytes, and $CD16^+$ monocytes were stimulated with 1 µg/ml LPS (Sigma-Aldrich) for 18 hours. All cell types were centrifuged at 500 x*g* for 5 minutes and 1,200 x*g* for 5 minutes followed by ultracentrifugation at 20,000 x*g* for 60 minutes at 4°C to pellet down the mMP.

Scanning electron microscopy (SEM) analysis

The morphology of mMP derived from monocyte subsets was assessed by FEI Quanta 450 Scanning Electron Microscope (SEM) (FEI). Monocytic MP of 20 µl were placed on the coverslips for 5 minutes. McDowell and Trump's fixative was used as a primary fixation at 4°C followed by washing with 0.1 M PBS. Samples were then post-fixed with 1% osmium tetroxide (OsO_4) (Sigma-Aldrich) for 1 hour at 4°C followed by dehydration by acetone (Sigma-Aldrich) gradual series: 50, 75, 95 and 100% at room temperature. The coverslips were immersed in 100% hexamethyldisilazane (HMDS) (Electron Microscopy Sciences) solution for 10 minutes at room temperature followed by air drying. A coating of 23 nm gold was applied by using a sputter coater (Leica) and viewed under a High Voltage (HV) of 5.00 kV and working distance (WD) of 10 mm. Images of mMP were viewed at 500× and 5000× magnifications. Monocytic MP were identified on SEM by standardised counting based on ten different selected areas within the same sample.

Dynamic Light Scattering (DLS) analysis

DLS measurement was performed by using NANOPHOX (Sympatec GmbH) equipped with a 10 mW He-Ne laser beam at a wavelength of 632.8 nm and 90° scattering angle at room temperature. The mMP were dispersed in 300 µl ultrapure water and measured directly without filtration. The measurement was performed using a 3D cross-correlation function of the scattering intensity, which was then analysed using cumulant analysis to obtain the hydrodynamic diameter of the mMP.

Statistical analysis

The data were analyzed using the Wilcoxon signed rank test and presented as median ± interquartile range (IQR). Values of $p < 0.05$ was considered statistically significant.

Results

Purified mMP samples from whole monocytes, $CD14^+$ monocytes and $CD16^+$ monocytes were subjected to SEM. By using the same magnification and working distance (WD), the morphology of all mMP appeared as fine, round shape in vesicle form (Fig. 1A). Besides, the populations of mMP also appeared as separate particles and aggregates.

The number of mMP was then calculated on ten different selected areas within the same sample performed on the SEM. The median number of mMP derived from LPS-stimulated whole monocytes were significantly higher compared to unstimulated mMP ($p < 0.05$) (Fig 1B). However, the number of mMP derived from $CD14^+$ monocytes and $CD16^+$ monocytes was not significantly different.

The size of mMP derived from whole monocytes, $CD14^+$ monocytes, and $CD16^+$ monocytes were then determined by DLS. The size of all mMP was approximately 140 nm in average and ranged between 100 to 200 nm (Fig 1C). Meanwhile, the mean polydispersity index (PDI) values of mMP derived from whole monocytes, $CD14^+$ monocytes, and $CD16^+$ monocytes were 0.0065 (Table 1).

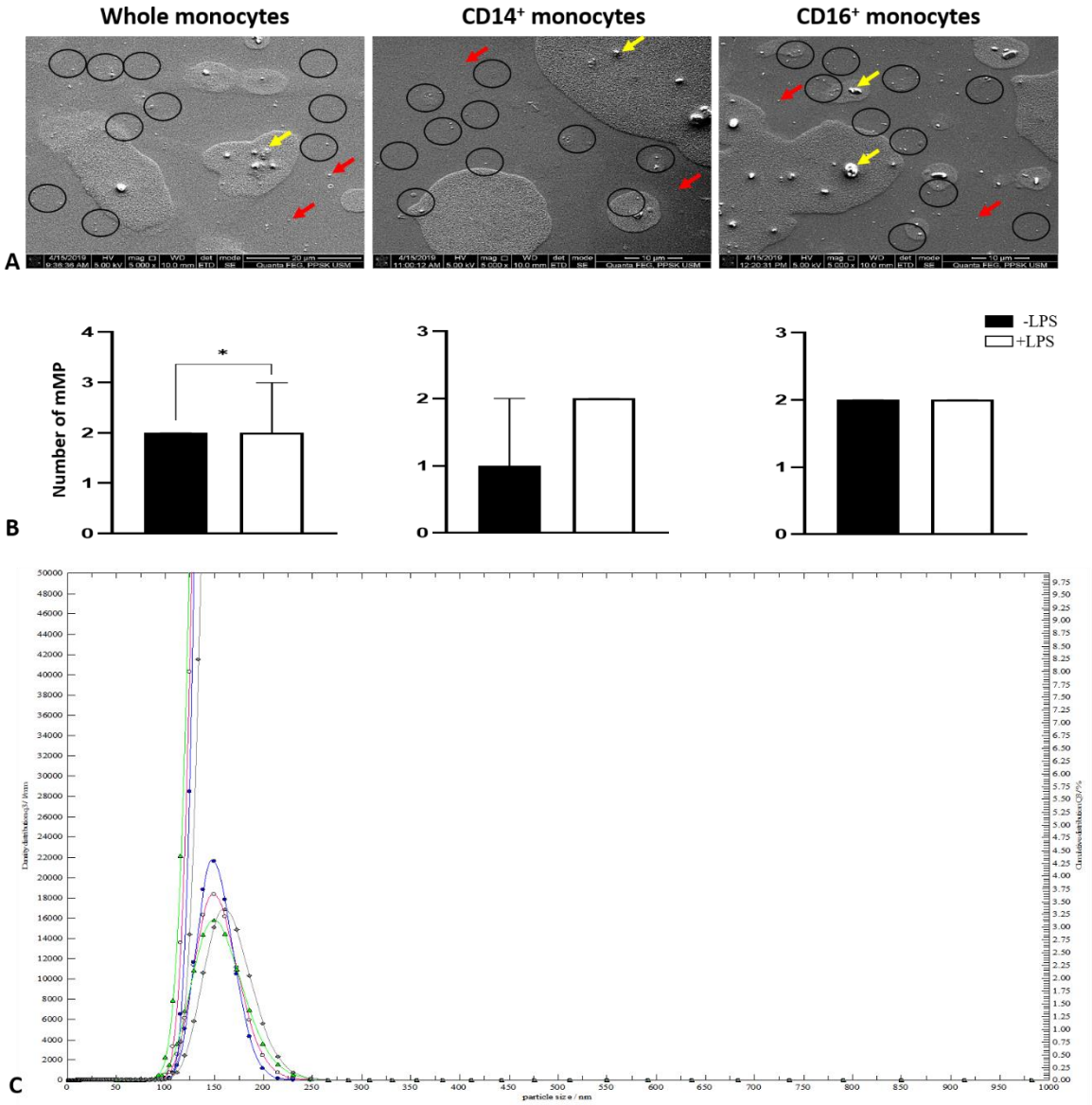

Fig. 1: The morphology and size of mMP as determined by SEM and DLS respectively. (A) mMP samples from whole monocytes, $CD14^+$ monocytes and $CD16^+$ monocytes were purified and subjected to SEM by using 5000× magnification. Red and yellow arrows indicate the round shape of mMP and aggregates of mMP, respectively. Populations of single mMP were gated in each image as shown by black circles. (B) The number of mMP derived from whole monocytes, $CD14^+$ monocytes, and $CD16^+$ monocytes were calculated based on ten different selected areas within the same sample. The graphs are expressed as median ± IQR. The indicated *p* values represent; $*p < 0.05$ (n=3). (C) The size of mMP derived from whole

monocytes, $CD14^+$ monocytes, and $CD16^+$ monocytes as determined by DLS. The plots are representatives of all mMP subtypes.

Table 1: Polydispersity index (PDI) of mMP

	Whole monocytes-derived mMP		**$CD14^+$ monocytes-derived mMP**		**$CD16^+$ monocytes-derived mMP**	
	-LPS	+LPS	-LPS	+LPS	-LPS	+LPS
Mean Size (nm)	129.6	154.8	118.6	127.5	115.6	124.8
SD	13.36	5.85	5.69	5.37	16.40	8.95
***PDI**	0.01	0.001	0.002	0.001	0.02	0.005

Notes: LPS=lipopolysaccharide; SD= standard deviation. *Mean = 0.0065

Discussion

The identification of morphology and size of mMP derived from different monocyte subsets has never been reported. In this study, mMP was generated from LPS stimulation of whole monocytes, $CD14^+$ monocytes and $CD16^+$ monocytes followed by differential centrifugations to isolate mMP. This method consists of sequential centrifugations, by increasing in speed and time to pellet particles which are decreasing in size [12]. In this study, initial centrifugation has successfully depleted cellular debris followed by additional centrifugation to remove apoptotic bodies. The supernatants collected by each centrifugations were subjected to ultracentrifugation at 4°C to recover the mMP [7]. All procedures were carried out at 4°C to maintain the functional properties of isolated mMP [13].

Immuno-affinity beads detection by fluorescence-activated cell sorting (FACS) allows the detection of individual mMP subpopulations but does not give an overall view of the mMP heterogeneous populations [14] and only offers a lower detection limit of approximately 300 to 500 nm [15]. Therefore, to precisely determine the size of mMP, direct imaging technique is preferred due to its intuitive high-resolution visualization of particles and the minimal influence of artefacts in size determination [16]. Electron microscopy has been considered as a standard imaging method for observing extracellular vesicles, including mMP [17] which was used in this study.

The images of mMP derived from whole monocytes, $CD14^+$ monocytes and $CD16^+$ monocytes were observed by SEM at 5000× magnification. Monocytic MP were mainly appear as round shape in vesicle form which is consistent with previous report [18]. However, some mMP also appear as separate particles as well as in aggregates. The aggregates may be due to sample preparation that involves fixation and dehydration which causes insignificant size or morphology alterations [19].

To correctly identify mMP population, the number of mMP in each SEM figure were only counted based on single appearance as round in shape rather than in aggregates. The number of mMP derived from LPS-stimulated whole monocytes were significantly higher

compared to unstimulated mMP. However, when the monocyte subsets were separated, the number of mMP obtained decreased. In an *in vivo* endotoxemia model, the number of monocyte subsets was reduced from the circulation following LPS stimulation possibly due to monocytes patrolling behaviour to the vessel walls [20]. However, the clear mechanism of how monocytes decrease during *in vitro* condition is unclear.

Dynamic light scattering (DLS) has been widely used to characterize the size and polydispersity of particles ranging in size between 3 to 7000 nm [21] which was used in this study. The average particle size of mMP measured using NANOPHOX analyser was approximately 140 nm which was within the size range of mMP. Accurate size distributions are expected for monodisperse samples, which are vesicles with only one size. Therefore in this study, Polydispersity Index (PDI) was used to estimate the average uniformity of a particle solution in which a particle is considered monodisperse when the PDI value is less than 0.1 [22]. All PDI values of mMP derived from whole monocytes, $CD14^+$ monocytes, and $CD16^+$ monocytes were less than 0.1. This suggests that mMP isolated by ultracentrifugation in our laboratory exhibit monodisperse property with no variation in particle size.

Conclusion

In conclusion, this is the first study that identify the morphology and size of mMP derived from human blood monocytes subsets. The morphology of mMP appear as round in shape as a single particle. The size of mMP was approximately 140 nm which is within mMP size range while the mean dispersity value was 0.0065 which suggests that mMP are monodisperse. Future study is recommended to accurately detect single mMP by particle number concentration rather than intensity.

Acknowledgment

This research was funded by Fundamental Research Grant Scheme (FRGS) Ministry of Education (MOE) Malaysia (Grant number: 203/PPSK/6171170). We thank the Scanning Electron Microscope Laboratory, School of Health Sciences, Universiti Sains Malaysia and Agensi Nuklear Malaysia for providing DLS service.

Author Contributions

Conceived and designed the study: MNRAM SZM NAB MA. Performed research: MNRAM SZM. Analyzed data: MNRAM NAB MA. Wrote the paper: MNRAM SZM NAB MA

Disclosure of Conflict of Interest

The authors declare no financial or commercial conflict of interests.

Compliance with Ethical Standards

The work is compliant with ethical standards.

References

[1] Halim, A.T.A., N.A.F.M. Ariffin, and M. Azlan, *the multiple roles of monocytic microparticles.* Inflammation, 2016. **39**(4): p. 1277-1284.

[2] Smalley, D.M., N.E. Sheman, K. Nelson, and D. Theodorescu, *Isolation and identification of potential urinary microparticle biomarkers of bladder cancer.* J Proteome Res, 2008. **7**(5): p. 2088-2096.

[3] Hugel, B., M.C. Martínez, C. Kunzelmann, and J.-M. Freyssinet, *Membrane microparticles: two sides of the coin.* Physiology, 2005. **20**(1): p. 22-27.

[4] Takeshita, J., E.R. Mohler III, P. Krishnamoorthy, J. Moore, W.T. Rogers, L. Zhang, J.M. Gelfand, and N.N. Mehta, *Endothelial cell-, platelet-, and monocyte/macrophage-derived microparticles are elevated in psoriasis beyond cardiometabolic risk factors.* J Am Heart Assoc, 2014. **3**(1): p. e000507.

[5] Ziegler-Heitbrock, L., *Blood monocytes and their subsets: established features and open questions.* Frontiers in immunology, 2015. **6**: p. 423.

[6] Sampath, P., K. Moideen, U.D. Ranganathan, and R. Bethunaickan, *Monocyte subsets: phenotypes and function in tuberculosis infection.* Front Immunol 2018. **9**.

[7] Crompot, E., M. Van Damme, H. Duvillier, K. Pieters, M. Vermeesch, D. Perez-Morga, N. Meuleman, P. Mineur, D. Bron, and L. Lagneaux, *Avoiding false positive antigen detection by flow cytometry on blood cell derived microparticles: the importance of an appropriate negative control.* PLoS One, 2015. **10**(5): p. e0127209.

[8] Ponomareva, A., T. Nevzorova, E. Mordakhanova, I. Andrianova, L. Rauova, R. Litvinov, and J. Weisel, *Intracellular origin and ultrastructure of platelet-derived microparticles.* J Thromb Haemost, 2017. **15**(8): p. 1655-1667.

[9] Maurer-Spurej, E. and K. Chipperfield, *Could microparticles be the universal quality indicator for platelet viability and function?* J. Blood Transfus, 2016. **2016**.

[10] Tahmasbi, L., M. Karimi, S.A. Kafiabadi, M. Nikougoftar, S. Haghpanah, R. Ranjbaran, and M. Moghadam, *Evaluation of Plasma Platelet Microparticles in Thrombotic Thrombocytopenic Purpura.* Ann Clin Lab Sci 2017. **47**(1): p. 62-67.

[11] Bernimoulin, M., E.K. Waters, M. Foy, B.M. Steele, M. Sullivan, H. Falet, M.T. Walsh, N. Barteneva, J.G. Geng, J.H. Hartwig, P.B. Maguire, and D.D. Wagner, *Differential stimulation of monocytic cells results in distinct populations of microparticles.* J Thromb Haemost, 2009. **7**(6): p. 1019-28.

[12] Abramowicz, A., P. Widlak, and M. Pietrowska, *Proteomic analysis of exosomal cargo: the challenge of high purity vesicle isolation.* Mol Biosyst 2016. **12**(5): p. 1407-1419.

[13] Théry, C., K.W. Witwer, E. Aikawa, M.J. Alcaraz, J.D. Anderson, R. Andriantsitohaina, A. Antoniou, T. Arab, F. Archer, and G.K. Atkin-Smith, *Minimal information for studies of extracellular vesicles 2018 (MISEV2018): a position statement of the International Society for Extracellular Vesicles and update of the MISEV2014 guidelines.* J. Extracell. Vesicles, 2018. **7**(1): p. 1535750.

[14] Ostrowski, M., N.B. Carmo, S. Krumeich, I. Fanget, G. Raposo, A. Savina, C.F. Moita, K. Schauer, A.N. Hume, and R.P. Freitas, *Rab27a and Rab27b control different steps of the exosome secretion pathway.* Nat. Cell Biol, 2010. **12**(1): p. 19.

[15] Robert, S., P. Poncelet, R. Lacroix, L. Arnaud, L. Giraudo, A. Hauchard, J. Sampol, and F. Dignat-George, *Standardization of platelet-derived microparticle counting using calibrated beads and a Cytomics FC500 routine flow cytometer: a first step towards multicenter studies?* J Thromb Haemost 2009. **7**(1): p. 190-197.

[16] Kim, A., W.B. Ng, W. Bernt, and N.-J. Cho, *Validation of size estimation of Nanoparticle tracking Analysis on polydisperse Macromolecule Assembly.* Sci. Rep, 2019. **9**(1): p. 2639.

[17] Hirsova, P., S.H. Ibrahim, A. Krishnan, V.K. Verma, S.F. Bronk, N.W. Werneburg, M.R. Charlton, V.H. Shah, H. Malhi, and G.J. Gores, *Lipid-induced signaling causes release of inflammatory extracellular vesicles from hepatocytes.* Gastroenterology, 2016. **150**(4): p. 956-967.

[18] Wu, Y., W. Deng, and D.J. Klinke II, *Exosomes: improved methods to characterize their morphology, RNA content, and surface protein biomarkers.* Analyst, 2015. **140**(19): p. 6631-6642.

[19] György, B., T.G. Szabó, M. Pásztói, Z. Pál, P. Misják, B. Aradi, V. László, E. Pállinger, E. Pap, and A. Kittel, *Membrane vesicles, current state-of-the-art: emerging role of extracellular vesicles.* Cell Mol Life Sci 2011. **68**(16): p. 2667-2688.

[20] Tak, T., R. van Groenendael, P. Pickkers, and L. Koenderman, *Monocyte Subsets Are Differentially Lost from the Circulation during Acute Inflammation Induced by Human Experimental Endotoxemia.* J Innate Immun, 2017. **9**(5): p. 464-474.

[21] Lawrie, A., A. Albanyan, R. Cardigan, I. Mackie, and P. Harrison, *Microparticle sizing by dynamic light scattering in fresh-frozen plasma.* Vox Sang, 2009. **96**(3): p. 206-212.

[22] Clayton, K.N., J.W. Salameh, S.T. Wereley, and T.L. Kinzer-Ursem, *Physical characterization of nanoparticle size and surface modification using particle scattering diffusometry.* Biomicrofluidics, 2016. **10**(5): p. 054107.